International Symposium
On Turbulence and Shear Flow
Phenomena (TSFP-9)
June 30 - July 3, 2015 *Melbourne, Australia*

FLOW PATTERN AND POLLUTANT DISPERSION OVER A THREE-DIMENSIONAL BUILDING ARRAY

Zhi Shen
Department of Engineering Mechanics
Tsinghua University
Beijing, China
shenzhi@tsinghua.org.cn

Bobing Wang
Department of Engineering Mechanics
Tsinghua University
Beijing, China
eugene_wbb@163.com

Guixiang Cui
Department of Engineering Mechanics
Tsinghua University
Beijing, China
cgx@mail.tsinghua.edu.cn

Zhaoshun Zhang
Department of Engineering Mechanics
Tsinghua University
Beijing, China
demzzs@mail.tsinghua.edu.cn

ABSTRACT

This paper investigates the flow pattern and pollutant dispersion in urban canopy by large eddy simulation of flow over an array of cubes. It has been found that the flow pattern can be categorized as five type based on the packing density, exemplified by the building separation, in comparison with the scales of flow over a isolated obstacle, characterized by a horseshoe-like external wake and an internal cavity. The five types of urban canopy flow are introduced as (1) Isolated roughness flow when the lateral and longitudinal building separations are much greater than the scales of external wake and internal cavity of flow over isolated roughness element; (2) External wake interference flow when lateral building separation is less than the lateral spacing of external wake of flow over isolated roughness element while the longitudinal building separation is greater than the longitudinal scale of internal cavity of flow over isolated roughness element; (3) Internal wake interference flow when the longitudinal building separation is in the same order of the size of internal cavity of flow over isolated roughness element; (4) Skimming flow when the both lateral and longitudinal building separations are less than the lateral and longitudinal scale of flow over isolated roughness element; (5) Street network flow when both lateral and longitudinal building separations are much less than the lateral and longitudinal scale of flow over isolated roughness element. Results of time-averaging velocity field and pollutant concentration contours are demonstrated for each type of flow patterns. It is concluded that the behavior of flow pattern and pollutant dispersion is governed by the packing density from a very low packing density, approximated as the flow around an isolated roughness element, to a high packing density, resembled as the network flow.

INTRODUCTION

The pollutant dispersion in urban atmosphere is an important topic in urban environment and has been paid great attention since late last century. For two dimensional urban canopies Oke (1988) proposed a street canyon model that the flow patterns over 2D street canyon depend on the ratio of the building separation of l to its height h. The flow regime is called isolated roughness if $l/h > 2$ (Fig.1a), wake interference if $l/h \sim 1$ (Fig.1b) and the flow is called skimming when $l/h < 1/2$ (Fig.1c). Since the pollutant dispersion is closely related to the flow patterns, the classification of flow regimes for 2D street canyon gives great help for understanding pollutant dispersion in real building canopy and casting engineering models (Walton *et al.*, 2002).

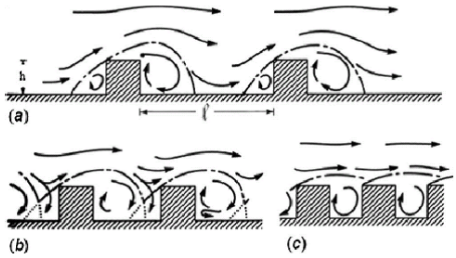

Figure 1. 2D street canopy (Oke, 1988)

However in real urban canopy the geometrical configuration is three dimensional and the flow patterns are different from those in 2D street canyon. For instance the flow pattern of 3D isolated roughness, shown in Fig.2 (Hanna *et al.*, 1982), is completely different from the flow pattern over 2D roughness elements (Fig.1a). Results of flow visualization(Martinuzzi & Tropea, 1993) indicate that there exist a horse shoe vortex around the roughness element and a pair of circulating flows behind the roughness element. In this case the pollutant will be entrained into the horse shoe vortex with high concentration if there is a pollutant source at the front of the roughness element. The purpose of this paper is to explore whether flow patterns can be classified to some identifiable regimes in 3D urban building canopy and to investigate the essential feature

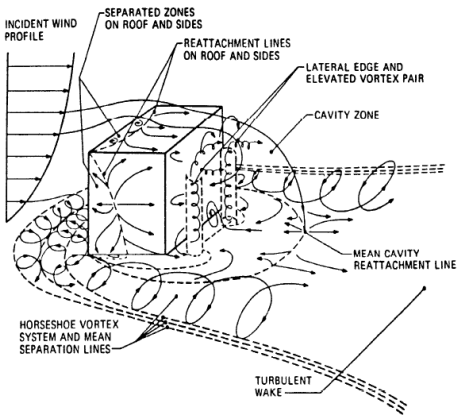

Figure 2. Flow pattern of 3D isolated roughness element (Hanna *et al.*, 1982)

of pollutant dispersion in the classifications. The LES is used in this paper for investigation of the flow patterns and pollutant dispersion. For easier computation and analyses the building canopy is simplified as cubic array while the buildings are fully resolved in computation. We have found that the separation of horse shoe vortex tails and the streamwise and lateral sizes of recirculation zone in the flow around a isolated roughness element (see Fig.2) are the key parameters controlling the behaviour of 3D building canopy flow of corresponding geometrical size, i.e. the roughness element height h. As a result the criteria of the classification are established based on the ratio between these characteristic scale and the geometrical parameters of urban building canopy.

NUMERICAL METHODS

The urban building canopy is simplified by the flow over an array of cubes. The incompressible Navier-Stokes equations and the transport equation for the passive scalar are discretized by finite volume method (FVM). The QUICK scheme is used in spatial discretization and the third order Runge-Kutta scheme is utilized for time advancement. The discretized equations are solved using the SIMPLE method on non-staggered grids with momentum interpolations. The air density $\rho = 1.208 kg\,m^{-3}$, and the kinetic viscosity coefficient $\nu = 1.5 \times 10^{-5} m^2 s^{-1}$. A constant longitudinal pressure gradient of u_τ^2/L_z is imposed to counterbalance the drag of buildings and the ground, where u_τ is the total wall friction velocity and L_z is the domain height. A point source will be inserted in the scalar equation.

In the lateral and longitudinal direction, the periodic boundary condition is applied for each velocity component, and the non-slip condition is applied at the building surface and ground. A free slip and impermeable condition is applied at the upper boundary. The concentration is set to zero at the inlet and lateral boundaries of the domain. The zero normal gradient of concentration is imposed at the outlet and the upper boundary as well as all the solid surfaces.

In each of the present simulations, the mesh has 12 grid points along each dimension of the cube mounted on the ground and is refined near the solid surface with the height of the first grid point of approximate $0.0037h$. Both the sub-grid viscosity and the sub-grid diffusivity are determined by the Lagrangian dynamic method(Meneveau *et al.*, 1996) respectively in the SGS model, hence the corresponding sub-grid Schmidt number $Sc_t = \nu_t/D_t$ is varying with local flow condition.

POLLUTANT DISPERSION IN THE CANOPY FLOW

Like the flow pattern of isolated roughness(see Fig.1a) in 2D street canyon, the 3D isolated roughness element is the simplest form of urban canopy in which the flow patterns are completely determined by the flow Reynolds number and the geometry of roughness. If the Reynolds number is high enough the flow is Reynolds number independent, or has so called self-similarity(Snyder, 1972). The peculiar feature of the flow pattern is that there exist a horse-shoe vortex around the lower part of the windward face and a leeward recirculation cavity in the flow over a isolated 3D roughness element (see Fig.2). The flow region containing the horse-shoe vortex is called the external wake area and the flow region inside the cavity is called the internal wake area.

In the following numerical simulations h equals $0.02m$,the velocity of free-stream flow U equals $10m/s$, and corresponding Reynolds number $Re(= Uh/\nu)$ is estimated of order 10^4. Based on the characteristic scale in the isolated roughness element flow, i.e. the width of external wake $W_e x$ and the scale of the internal wake h(Schulman *et al.*, 2000), the flow pattern in 3D building canopies can be classified into the following five types.

Isolated roughness regime

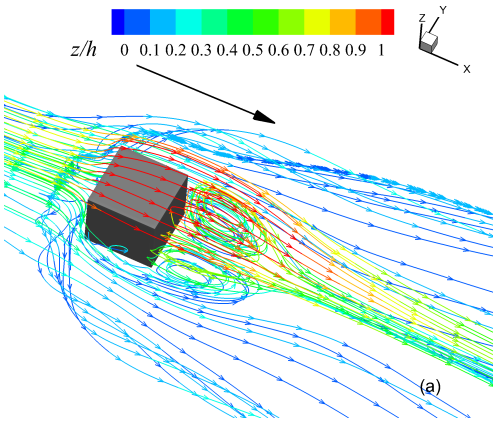

Figure 3. The streamlines around isolated 3D roughness element by present computation

The first type of 3D canopy flow is defined as isolated roughness when the lateral building separation $W_L \gg W_{ex}$ and the streamwise separation $W_S \gg h$. In this case the neighbouring buildings do not influence the flow around each individual building and the flow pattern is similar to that over an isolated roughness element. The boundary conditions of velocities are different from as mentioned above to those in this case of flow around a isolated cube.

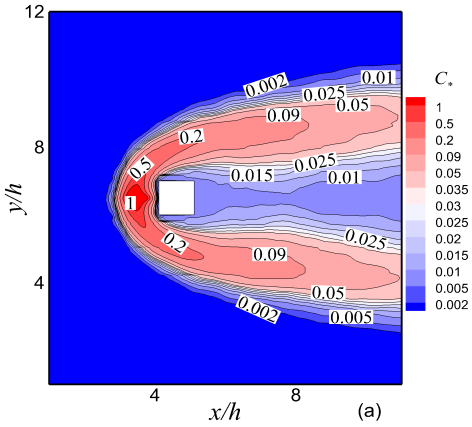

Figure 4. Horizontal distribution of pollutant in isolated roughness flow. The same contour level is applied in all the following pollutant distributions

The inflow data is generated synchronously according to Xie & Castro (2008). The normal gradient of each velocity component u,v,w is set to zero at the outlet with flux correction. A point pollutant source is located in front of the roughness element with streamwise distance $x = 0.5h$ and $z = 0.05h$ from the ground. The streamlines of time-averaging velocity field is presented in Fig.3 and consist of a external wake and a internal wake as mentioned above. Fig.4 display a distinct double-peak distribution in the lateral direction and indicates that the pollutant is mainly distributed in the horse vortex region.

External wake interference regime

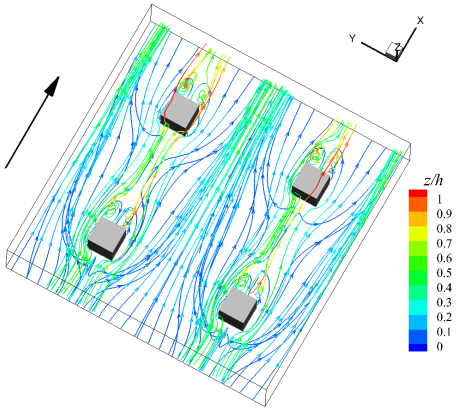

Figure 5. Streamlines in external wake interference flow

When the lateral distance between buildings is less than length of external wake ($W_L < W_{ex}$) whereas longitudinal distance still much larger than length of near wake ($W_S \gg h$), the flow over building canopy is called external wake interference. In this case the individual building can no longer be viewed as isolated. The external wake of each individual building, i.e. the horse shoe vortex, interacts with that of neighbouring buildings, while the internal wake is not affected by neighbouring buildings. An

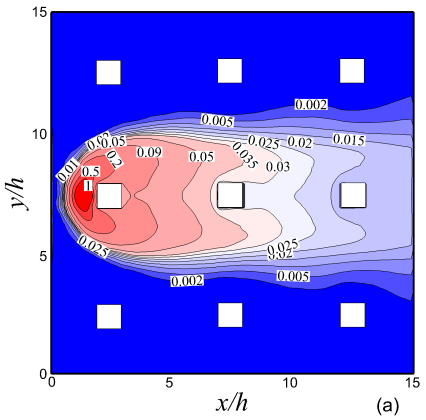

Figure 6. Horizontal distribution of pollutant in external wake interference flow

example of this flow regime is illustrated in Fig.5 in which flow is simulated numerically over an array of cubes with both streamwise and spanwise separation of the roughness element equaling $4h$.

Fig.6 illustrates the distribution of pollutant concentration for external wake interference flow on a horizontal section. The point source is located in the head region of horse shoe vortex; however the pollutant is not concentrated in the horse vortex region but spread in to the internal wake region because the separation of horse vortex tails is narrower. Fig.6 clearly shows this pattern.

Internal wake interference

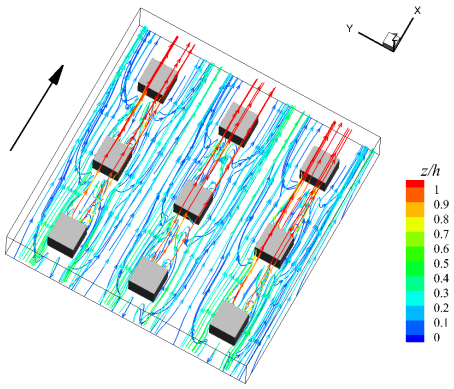

Figure 7. Streamlines in internal wake interference flow

When the streamwise separation of buildings is in the same order of the longitudinal size of internal wake, that is $W_s \sim h$, the flow pattern is named internal wake interference flow. A case with both streamwise and spanwise distances between buildings equalling $2h$ simulated to represent such kind of flow. As viewed from streamlines in Fig.7, the external wake is similar to the last case while the internal wake of each building is influenced by the downwind building.

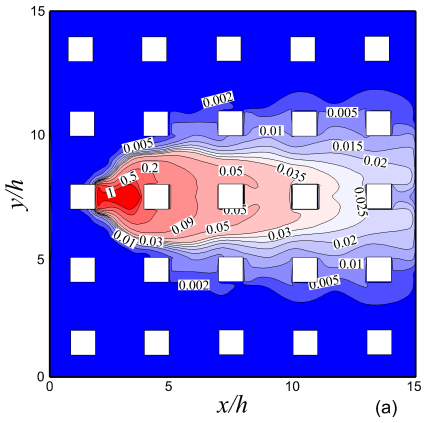

Figure 8. Horizontal distribution of pollutant in internal wake interference flow

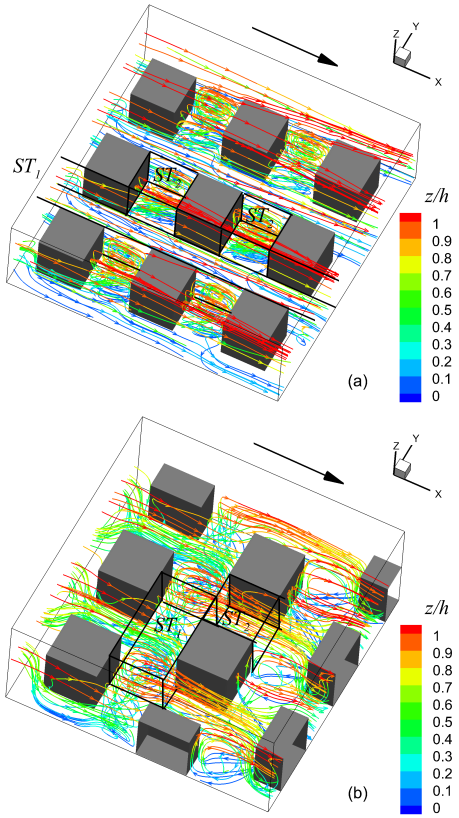

Figure 9. Streamlines in the skimming flow. (a)Non-staggered (b)Staggerd

Fig.8 illustrates distribution of pollutant concentration for internal wake interference flow on horizontal cross-sections. The pollutant spreads quickly to neighbouring columns, which is different from dispersion in external wake interference flow. As shown in Fig.8, although the point source is located before the second row, there is high concentration region behind first row because the pollutant released from source is trapped in the internal wake region of forward building.

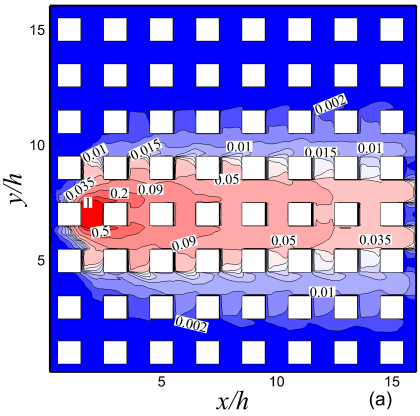

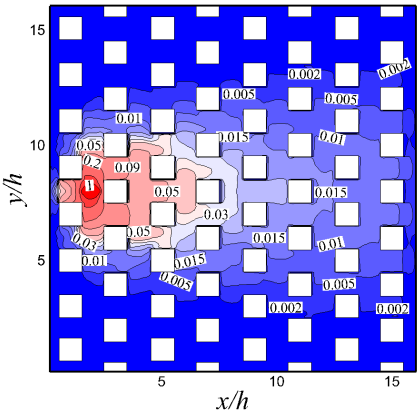

Figure 10. Horizontal distribution of pollutant in the skimming flow. (a)Non-staggered (b)Staggerd

Skimming flow

If the building separation is further decreasing that both longitudinal and lateral spacing equal h, then both internal and external wakes are restricted. This case is named skimming flow and in this case two different layouts of buildings are investigated corresponding to stagger and non-stagger arrangements of buildings, see Fig.9a and Fig.9b. The difference between 3D and 2D skimming flows can be clearly shown in the distribution of pollutant concentration. In both staggered and non-staggered case the external and internal wakes do not exist anymore due to the large packing density and the flow is at high speed over building canopy with low speed circulation inside canopy. This is similar to 2D street canyon; however the flow is three dimensional inside canopy.

Fig.10 presents the pollutant concentration in the skimming flow. The pollutant is transported in streamwise direction and dispersed in lateral direction. The pollutant dispersion in 3D skimming is similar to 2D skimming flow only in the central section at $(y-y_s)/h=0$. Comparison between Fig.10a and Fig.10b indicates that the pollutant concentration is lower inside building canopy in staggered case due to the strong dispersion.

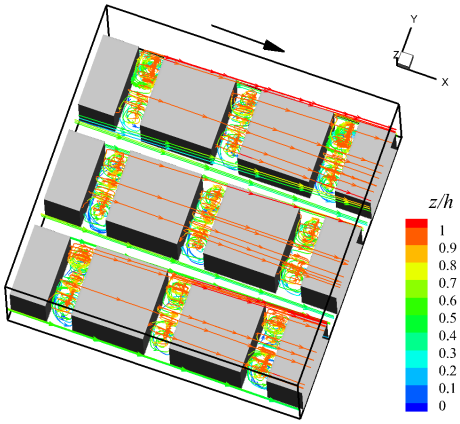

Figure 11. Streamlines in street network flow

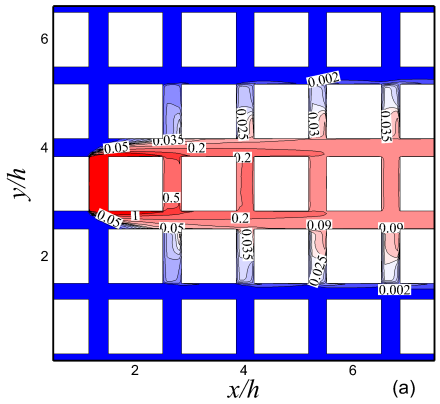

Figure 12. Horizontal distribution of pollutant in street network flow

Street network

When the spacing between buildings is much less than the building height, the flow in the canopy looks like in a network that both external and internal wakes disappears and it can be called street network. The street network is somewhat simpler building canopy and has been studied by Hamlyn *et al.* (2007) and Soulhac *et al.* (2011). Fig.11 shows the flow pattern in street network where the flow in the streets parallel to the free-stream direction can be simplified as channel flow while the flow in the street perpendicular to the free-stream direction looks like skimming flow in street canyon. The pollutant dispersion is demonstrated in Fig.12 for simple street network. The point source is dispersed downstream and gradually decaying, while it is dispersed only into neighbouring street. The reason for this simple case is easily understood. When the flow over the street network in oblique direction the flow pattern is more complicated, Hamlyn *et al.* (2007) and Soulhac *et al.* (2011) proposed a model for general street network flow; it is an engineering model for quick estimate the pollutant dispersion by simple flow and dispersion principles, for instance the flow continuity and well mixing assumption. We will not introduce the street network model in this paper, the more detailed description and prediction approach can be found elsewhere (Hamlyn *et al.*, 2007, Soulhac *et al.*, 2011). We just emphasize that the street network is one of the classification of building canopy that the streamwise and lateral separation between buildings is much less than the building height, i.e. $W_S \ll h$ and $W_L \ll h$.

DISCUSSION AND CONCLUSION

In summary the flow patterns and pollutant dispersion can be identified as five regimes which depend on the geometrical parameters of building canopy and characteristics of flow over isolated roughness element. The essential feature of different flow patterns is the building wake effect which is varying with the building density. For low building density the flow is approximated to isolated roughness element and the pollutant dispersion is governed by the downwash effect of the building wake (Schulman *et al.*, 2000). For high building density the flow is approximated to quasi two dimensional and the street network model (Hamlyn *et al.*, 2007, Soulhac *et al.*, 2011) is appropriate. The external wake interference and internal wake interference flows are 3D complex turbulent flow, the characteristics of pollutant concentration are varying with the building density. Therefore practical model for these two flow types is expected to be reconstructed after more detailed quantitative study.

Acknowledgements

The authors are funded by Chinese NSFC (grant number 1132005,11002081) and the supercomputing is supported by Tsinghua National Laboratory of Information Science and Technology and the Beilong Super-cloud Computing co., LTD, Beijing .

REFERENCES

Cheng, W. C. & Liu, C. H. 2011 Large-eddy simulation of turbulent transports in urban street canyons in different thermal stabilities. *Journal of Wind Engineering and Industrial Aerodynamics* **99** (4), 434–442.

Hamlyn, D., Hilderman, T. & Britter, R. 2007 A simple network approach to modelling dispersion among large groups of obstacles. *Atmospheric Environment* **41** (28), 5848–5862.

Hanna, S.R., Briggs, G.A. & Hosker, R.P. Jr. 1982 Handbook on atmospheric diffusion. BOOK DOE/TIC-11223; Other: ON: DE82002045 United States10.2172/5591108Other: ON: DE82002045Thu Feb 07 00:13:37 EST 2008NTIS, PC A06/MF A01.TIC; NTS-82-008222; ERA-07-038976; EDB-82-097032English. U.S. Department of Energy DOE/TIC-11223,.

Martinuzzi, R. & Tropea, C. 1993 The flow around surface-mounted, prismatic obstacles placed in a fully-developed channel flow. *Journal of Fluids Engineering-Transactions of the Asme* **115** (1), 85–92.

Meneveau, C., Lund, T. S. & Cabot, W. H. 1996 A lagrangian dynamic subgrid-scale model of turbulence. *Journal of Fluid Mechanics* **319**, 353–385.

Oke, T. R. 1988 Street design and urban canopy layer climate. *Energy and Buildings* **11** (1-3), 103–113.

Schulman, L. L., Strimaitis, D. G. & Scire, J. S. 2000 Development and evaluation of the prime plume rise and building downwash model. *Journal of the Air & Waste Management Association* **50** (3), 378–390.

Snyder, W. H. 1972 Similarity criteria for the application of fluid models to the study of air pollution meteorology. *Boundary-Layer Meteorology* **3** (1), 113–134.

Soulhac, L., Salizzoni, P., Cierco, F. X. & Perkins, R. 2011 The model sirane for atmospheric urban pollutant dispersion; part i, presentation of the model. *Atmospheric Environment* **45** (39), 7379–7395.

Walton, A., Cheng, A. Y. S. & Yeung, W. C. 2002 Large-eddy simulation of pollution dispersion in an urban street canyon - part i: comparison with field data. *Atmospheric Environment* **36** (22), 3601–3613.

Xie, Z. T. & Castro, I. P. 2008 Efficient generation of inflow conditions for large eddy simulation of street-scale flows. *Flow Turbulence and Combustion* **81** (3), 449–470.

Xie, Z. T., Coceal, O. & Castro, I. P. 2008 Large-eddy simulation of flows over random urban-like obstacles. *Boundary-Layer Meteorology* **129** (1), 1–23.